Heat Transfer Enhancement on Surface with Jets Impingement from Some Arrays of Elongated Round Orifices

Makatar Wae-hayee[1], Perapong Tekasakul[1], Chayut Nuntadusit[*1]

1. Energy Technology Research Center and Department of Mechanical Engineering,
Faculty of Engineering, Prince of Songkla University, Hatyai, Songkhla, Thailand
*Corresponding Author's E-mail: chayut@me.psu.ac.th

Abstract

The aim of this research is to enhance the heat transfer on a target surface of an array of impinging jets by decreasing effect of crossflow. Conventional round orifices (Aspect Ratio, AR=1) were substituted by elongated round orifices with aspect ratio AR=4 and 8 in base on same jet exit area. Two types of orifices arrangement; in-line and staggered arrangement were considered. The experimental investigation was carried out at constant distance from orifice plate to impinged surface $H=2D_E$ (D_E is equivalent diameter of orifice). The heat transfer characteristic was visualized using Thermochromic liquid crystal sheet (TLCs) and Nusselt number distribution was evaluated by image processing techniques. The flow characteristic on the impinged surface was also visualized by oil film technique. The results show that the elongated round orifices with AR=4 can increase average Nusselt number more than case of AR=1 for 6.04% and 12.52% in case of in-line and staggered arrangement, respectively. However, the heat transfer for case of AR=8 was enhanced only for in-line arrangement when compared with the case of AR=1. The results from flow visualization on jets impinged surface show that the jets from elongated round orifices with AR=4 were received crossflow effect smaller than jets from orifices with AR=1 and 8.

Keywords*:* Impinging jets, Crossflow, Heat transfer enhancement, Elongated round orifice, Orifices arrangement

1. Introduction

Impinging jets are widely used in many industrial applications which required high heat transfer rate on surface such as cooling of gas turbine blade, electronic device or wall of combustion chamber. However, the heat transfer rate is high only in jet directly impinging region. When the high and uniform heat transfer distribution is required over a wide area for example: drying of film sheet, heating of steel sheet, multiple or array of impinging jets is usually instead. An important parameter that influences on the multiple of jet impingements in a confined space is the crossflow. Here, the crossflow is defined as the fluid flow in the direction perpendicular to the jet impingement flow [1]. The crossflow was produced by

accumulating of spent jets from upstream to downstream of the confined space.

Katti and Prabhu [1] studied the effect of jet-to-jet distance and jet-to-plate distance on heat transfer rate in case of round impinging jets with in-line arrangement. They concluded that the jet-to-jet distance at S=4D give higher heat transfer rate than case of S=2D and 6D (D is nozzle diameter). And jet-to-plate distance at H=1D and 2D are better than case of H=3D.

Brizzi et al. [2] illustrated the flow and temperature patterns on the impinged surface of array of round jets with an in-line arrangement. The results of the flow pattern corresponded to the temperature pattern. And crossflow deforms significantly the impingement area that located at downstream in confined channel.

Previous studies [1-4] have been investigated heat transfer characteristics on jet impingement surface with crossflow. They concluded that the crossflow reduced significantly the heat transfer on impingement surface at downstream [3]. The aim of this research is to increase the heat transfer on the impinged surface by reducing the effect of crossflow in case of low jet-to-plate distance $H=2D_E$. Elongated round orifices with AR=4 and 8 were studied compare with conventional round orifices (AR=1). The jet Reynolds number for each orifice was kept constant at Re=13,400. Two type of jet flow arrangement; an in-line and staggered arrangement were also investigated. The comparisons of flow and heat transfer characteristics on the impinged surface are based on the constant jet mass flow rate.

2. Experimental Model

The experimental model is shown in Fig. 1. The multiple jets are discharged from array of orifices the round orifices, and impinge normal to opposite surface in a confined rectangular duct. The crossflow is then generated by accumulating the jets impinged air at upstream side and finally flow out to exit at one side of the duct. It should be noted that the velocity of crossflow increase as going downstream near the flow exit. The impinging jets in last column near the flow exit affected the strongest cross flow effect. The jet-to-plate distance is $H=2D_E$.

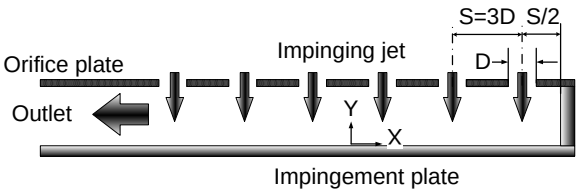

Fig. 1. Experimental model of array of jets impingement

The details of orifice geometry which used in this study are shown in Fig.2. All orifices have same exit area (about 136.8 mm^2). In this study, the equivalent diameter D_E is defined as diameter of round orifice which has same exit area and D_E is equal to 13.2 mm.

Round orifice Elongated round orifice

	L (mm)	W (mm)
AR=1	13.2	13.2
AR=4	24	6
AR=8	33.6	4.2

Fig. 2. Orifice geometry with identical cross-section area

Fig.3 illustrates the arrangements of array of jets; the in-line and staggered arrangement. Both arrangements have same number of 6x4 jet holes. The jet-to-jet distance was fixed at S=3D. The confined walls for each arrangement were fixed at location as shown in Fig. 3.

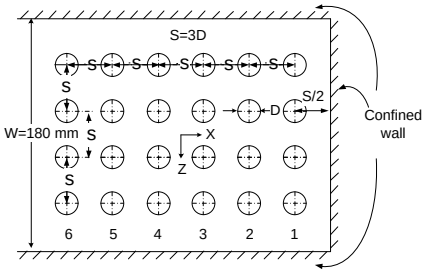

(a) In-line arrangement

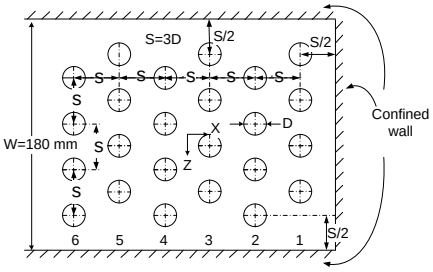

(b) Staggered arrangement

Fig. 3. Jet arrangement (No.1 to 6 represente the number of jets column)

3. Experimental Setup and Method

3.1. Experimental setup

Fig.4 shows schematic diagram of the experimental apparatus. The blower (3HP) was used for generating the air jets. The air flows through a temperature controlled chamber and towards the orifice flow meter. The air subsequently passes through a jet chamber with constant cross-section 360 mm x 360 mm and 850mm in height. The jet chamber was equipped with two of perforated plates and two of mesh plates to ensure uniform flow approached to the orifice plate. For all experimental conditions, the air flow rate was controlled at constant flow. The Reynolds number of each jet is constant at Re=$V_j D/\nu$ =13,400. The jet temperature was measured in jet chamber and controlled at T_j=27.0^{o}C during experiment.

3.2. Heat transfer measurement

Fig. 4 shows the detail of test section for heat transfer measurement. The test section was mounted upon the jet chamber. The air jets were discharged from orifice plate, and then impinged upon the electrical heated surface for cooling. The heat transfer surface was made of stainless steel foil (30-μm-thickness) which attached with TLC sheet (Omega Engineering, LCS-95) on the rear side of jet impinged surface. The stainless steel foil was stretched between couple of copper bus bars. The heat transfer surface was heated by DC power supply that can supply current up to 50A passes through copper bus bars. An amount of electrical energy is dissipated in the stainless steel foil and is calculated from equation

$$\dot{Q}_{input} = I^2 \cdot R \qquad (1)$$

where here, I is the electrical current and R is the electric resistance of stainless steel foil.

The local heat transfer coefficient (*h*) can be evaluated from equation

$$h = \frac{\dot{Q}_{input} - \dot{Q}_{losses}}{A(T_w - T_j)} = \frac{\dot{q}_{input} - \dot{q}_r - \dot{q}_c}{T_w - T_j} \qquad (2)$$

where $\dot{q}_r = \sigma \varepsilon_{TLC} (\overline{T_w}^4 - T_s^4)$ and $\dot{q}_c = \overline{h_c}(\overline{T_w} - T_s)$ are the heat loss transferred to the environment by radiation and convection, respectively. Here, $\overline{T_w}$ and T_j are average wall temperature and jet temperature, σ is a Stefan-Boltzman constant, ε_{TLC} is an emissive coefficient of TLCs (=0.9) [4]. T_s is surrounding temperature and $\overline{h_c}$ is natural heat transfer coefficient for heat loss from the TLC to the surrounding air.

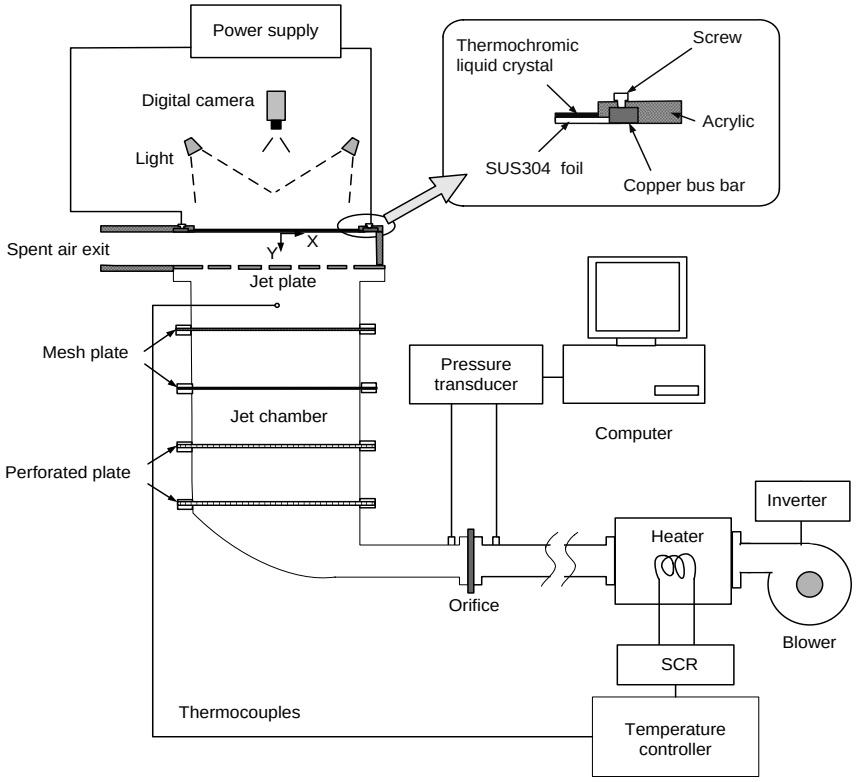

Fig. 4. Schematic diagram of the experimental setup

The wall temperature (T_w) on the impinged surface was measured by using TLC sheet that attached on the rear side of jet impinged surface. The CCD camera was used to capture color patterns on TLC sheet. The images of color pattern were converted from the RGB (Red, Green and Blue) color system to the HSI (Hue, Saturation and Intensity) color system. The Hue (H) value was used to correlate the color of TLC to their temperature in range of 28-40°C via calibration experiments. The TLCs was calibrated with same conditions with experiment to keep all external factors constant. The local Nusselt number was calculated from

$$Nu = \frac{hD_E}{k} \quad (3)$$

where, D_E is the equivalent diameter of orifice and k is a conductivity of air jet.

An average Nusselt number was calculated from

$$\overline{Nu} = \frac{\bar{h}D_E}{k} \quad (4)$$

where here, the average heat transfer coefficient $\bar{h}$ was calculated from Eq.(2) by replacing T_w to $\overline{T_w}$.

3.3. Flow visualization on the impinged surface

The flow visualization on the impinged surface was illustrated by using oil film technique. The oil film was prepared by mixing liquid paraffin, titanium dioxide and oleic acid. A transparent plastic plate was used for jet impinged wall and painted by oil film uniformly. The CCD camera was used to record oil film pattern on the impinged surface every 30 seconds.

4. Results and Discussions

4.1 Flow patterns on an impinged surface

The flow visualization on the impinged surface is shown in Fig. 5. The black area and white area represent area of oil film removed completely from wall and area of wall with oil film coating, respectively. A white points in the middle of black areas represent the stagnation point of jet bounded by jet impingement region. The black dots are the location of center of each orfices. The flow patterns of both in-line and staggered arrangement illustrated that the impingement region at downstream (column No. 4-6) moved to downstream by crossflow. Pattern in jet impingement regions depend on the location on jets and jet arrangement.

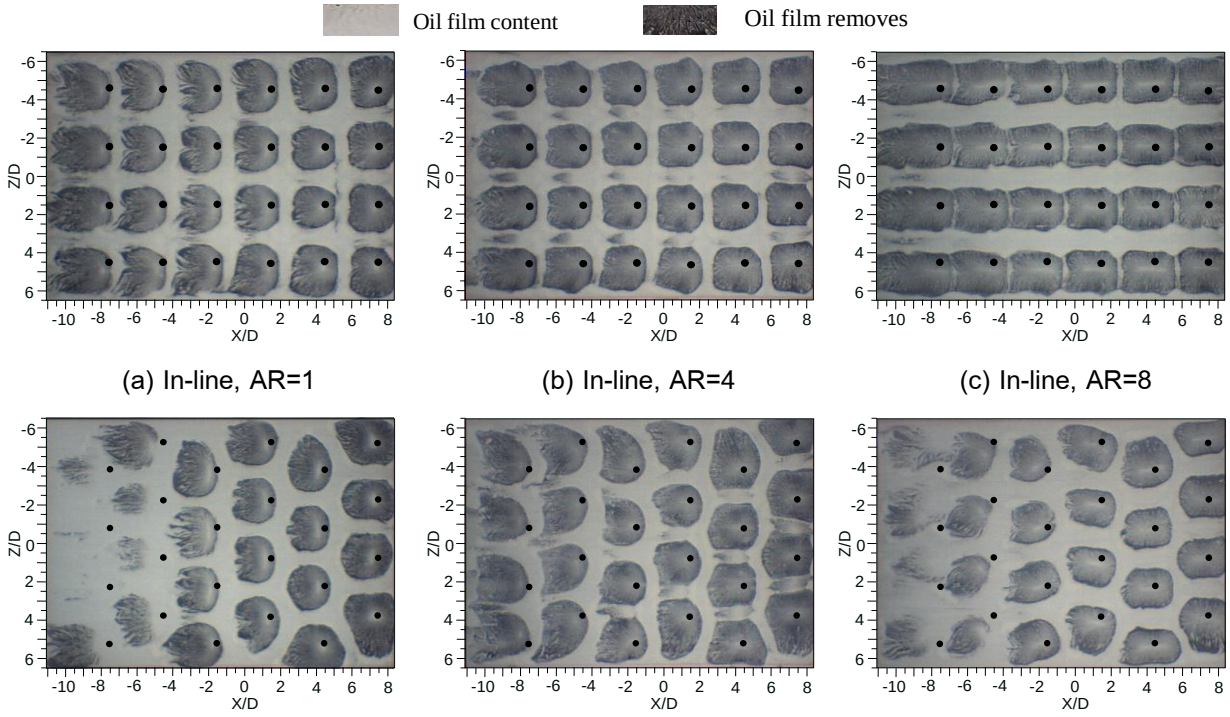

(a) In-line, AR=1 (b) In-line, AR=4 (c) In-line, AR=8

(d) Staggered, AR=1 (e) Staggered, AR=4 (f) Staggered, AR=8

Fig. 5. Flow patterns on the impinged surface (Re=13,400, black dot represents the center of each orifice)

In the case of in-line arrangement (Fig. 5. (a)-(c)), the charachteristic of stagnation regions are different depending on orifice geometry. The stagnation regions of elongated round orifice jet are more extended to crossflow direction, as increase AR, especially, in case of the AR=8. The stagnation regions for AR=1 (Fig.5 (a)) depends on location of jets, the stagnation regions more moved to the downstream for the jets that located far away from column No.1. However, the movement of impingement region for elongated round orifices (Fig. 5. (b) and (c)) are smaller than case of AR=1 (Fig. 5. (a)). This means that the elongated round orifices for both AR=4 and 8 can decrease the effect of crossflow to impinging jets.

In case of AR=1 with staggered arrangement (Fig. 5. (d)), the stagnation regions of jets that located in upstream region (column No. 1-3) are more clearly expresse than of the jets that located in downstream region (column

No. 4-6). Due to the confined wall, the impinging jets in downstream area affected the strong crossflow by accomulating spent jets from upstream. So that, the jets that located at downstream region (column No. 4-6) are mixing strongly with crossflow and lose momentum for impinging on target surface. It is contrast from case of in-line arrangement (Fig. 5 (a)). It shows that the stagnation regions are slightly different between upstream and downstream region. Because, the spent jets can passes easily through the channel between the rows of jets. So, the crossflow effect on impinging jets becomes small.

In case of AR=4 with staggered arrangement (Fig. 5. (e)), the stagnation regions at downstream region (column No. 4-6) are clearer than case of the AR=1 (Fig. 5. (d)). Because, the effect of crossflow on jets from orifices case of AR=4 is weaker than case of AR=1. However, the stagnation regions at downstream region for case of AR=8 are unclear as same as case of AR=1. Since, the orifice with AR=8 is slim and the circumference of this orifice jet which contact with crossflow is larger than case of AR=4, so the mixing between jet and crossflow is more than case of AR=4. The momentum of jet impinged on ther target surface is smaller than case of AR=4.

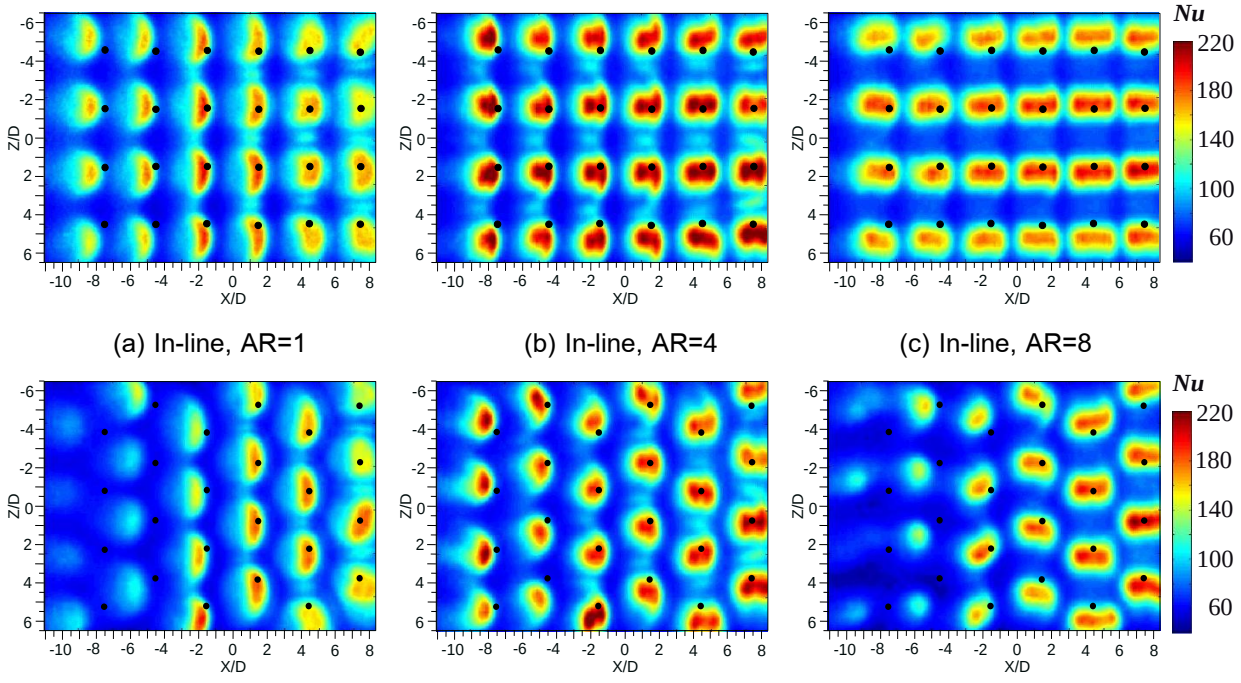

(a) In-line, AR=1 (b) In-line, AR=4 (c) In-line, AR=8

(d) Staggered, AR=1 (e) Staggered, AR=4 (f) Staggered, AR=8

Fig. 6. Nusselt number distribution on the impinged surface (T_j=27°C, Re=13,400, black dot represents the center of orifice)

4.2 The local Nusselt number on the impinged surface

The Nusselt number distributions on the impinged surface are shown in Fig. 6. The characteristic of heat transfer corresponded the flow pattern on the impinged surface (Fig.5) with same experimental condition. The Nusselt number in stagnation regions for case of AR=4 and 8 with in-line arrangement is higher than of AR=1. The area of high heat transfer for AR=4 and 8 are extended in crossflow direction corresponding to the orifice geometry.

The Nusselt number characteristic of the staggered arrangement is contrast with case of the in-line arrangement. The Nusselt number in upstream region (column No. 1-3) for case of staggered arrangement is high, but decrese rapidly as going downstream (column No. 4-5). Except for case of AR=4, the Nusselt number decreses gradually when compare with the upstream area of itself. The impinging jets from orifices case of AR=4 can increase heat transfer for both in-line and staggered arrangement. But, the impinging jets from orifices at AR=8 can increase heat transfer only for in-line arrangement. The reason has been discussed in flow visualization results.

Fig. 7 (a) shows the local Nusselt number distribution along Z/D=0 and 1.5 for the in-line arrangement. The results show that impinging jets from orifices at AR=4 give highest peak of Nusselt number. However, it is lower than case of AR=8 in area between the column of jet. The high heat transfer compensate from the stagnation region to area of between the column of jet for case of the AR=8, so the peak of Nusselt number at stagnation region for AR=4 is higher than of AR=8. In addition, the Nusselt number at area of between the rows of jet (dash line) for AR=8 are lowest.

Fig. 7 (b) shows the local Nusselt number distribution along Z/D=2.25 for staggered arrangement. The peak of Nusselt number is only high in upstream region (column No. 1-3) and decrease as going downstream (column No. 5). Except for case of AR=4, the peak of Nusselt number is still high in downstream region.

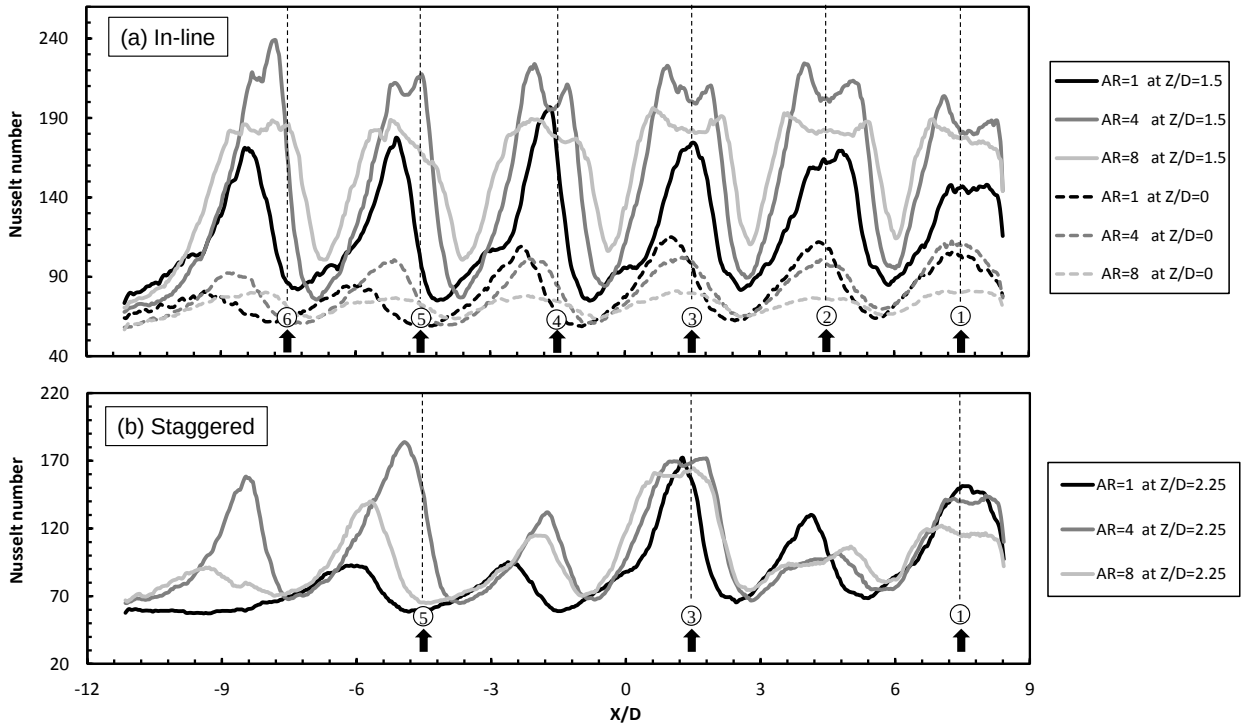

Fig. 7. Local Nusselt number distribution along crossflow direction (T_j=27°C, Re=13,400)

4.3 Average Nusselt number

The average Nusselt number on the impinged surface was calculated by using average temperature in area of -6.5<Z/D<6.5 and -11.15<X/D<8.4. The results for each orifice geometry and arrangements are compared in Fig. 8. The elongated round orifice can increase heat transfer rate on impingement region. The average Nusselt number of the in-line arrangement is higher than case of staggered arrangement for all of AR. The average Nusselt number for AR=4 with in-line arrangement is highest and slightly higher than case of AR=8. In case of in-line arrangement, the average Nusselt number for both case of AR=4 and 8 are higher 6.04 % and 5.54 % than case of AR=1. However, for the staggered arrangement, only average Nusselt number for case of AR=4 is higher 12.52% than of AR=1, but for case of AR=8, the average Nusselt number is smaller when compare with case of AR=1.

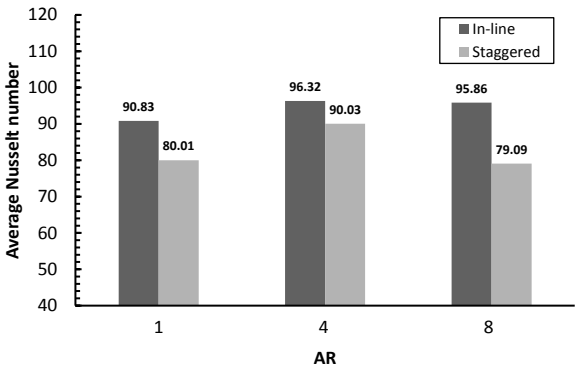

Fig. 8. Average Nusselt number

5. Conclusions

In present study, the effects of orifice geometry and jet flow arrangement were experimentally investigated. The main results were shown as follows;

(1) The impinging jets from elongated round orifices AR=4 can decrease effect of crossflow for both in-line and staggered arrangement, so

the heat transfer rate for both jet arrangement is higher than case of AR=1 and 8.

(2) The AR=8 can increase the heat transfer in stagnation region and area between columns of jet for in-line arrangement, but it is rapidly decrease in downstream region for staggered arrangement.

(3) The average Nusselt number of the in-line arrangement are higher than of staggered arrangement for any AR, and the average Nusselt number for AR=4 is the highest.

Acknowledgement

This research was sponsored by Faculty of Engineering, Prince of Songkla University through grant No. ENG-53-2-7-02-0070-S.

References

[1] Katti, V. and Prabhu, S. V. (2008), Influence of spanwise pitch local heat transfer distribution for in-line arrays of circular jets with air flow in two opposite, *Experimental Thermal and Fluid Science J.*, vol. 33, pp. 84 – 95.

[2] Brizzi, L.E., Bernard, A., Bousgarbies,J. L., Dorignac, E. and Vullierme, J. J. (2000), Study of several impinging jet, *Thermal Science J., v*ol. 9 (3), pp. 217 – 223.

[3] Bouchez, J.P. and Goldstein, R.J. (1975), Impingement cooling from a circular jet in a crossflow, *Heat and Mass Transfer Int. J.,* vol. 18, pp. 719 – 730.

[4] Geers, L.F.G., Tummers, M.J., Bueninck, T.J. and Hanjalic, K. (2008), Heat transfer correlation for hexagonal and in-line arrays of impinging jets, *Heat and Mass Transfer Int. J.*, vol. 51, pp. 5389 – 5399.